

**Ferromagnetism in iron-chromium alloys. II. Neutron scattering studies\***

A. T. Aldred

*Argonne National Laboratory, Argonne, Illinois 60439*

B. D. Rainford

*Imperial College, London, England*

J. S. Kouvel

*University of Illinois, Chicago, Illinois 60680*

T. J. Hicks

*Monash University, Clayton, Victoria, Australia*

(Received 19 January 1976)

Diffuse neutron scattering measurements have been made on ferromagnetic iron-chromium alloys containing 15-, 30-, 50-, and 73-at.% Cr with the long-wavelength neutron spectrometer at Harwell. The results have been analyzed, within the framework of the Marshall model, to determine both the average moments at the iron and chromium sites and the disturbances in the individual moments arising from fluctuations in the near-neighbor environment. The average moment per iron atom rises to a small maximum around 15-at.% Cr and then decreases as the chromium concentration increases. The average chromium moment is negative and becomes smaller in magnitude as the chromium concentration increases. The sum of the disturbances at the iron and chromium sites changes sign as a function of concentration. The range of the disturbance appears to be smaller in chromium-rich than in iron-rich alloys.

## I. INTRODUCTION

The use of long-wavelength, low-angle neutron scattering techniques to study the spatial variation of magnetic moment from atom to atom in ferromagnetic alloys was pioneered by Low and his associates at Harwell.<sup>1</sup> Their experiments were primarily used to study disturbances in the atomic magnetic moment around impurities (in concentrations of 1–2 at.%) in iron and nickel. In particular, the effect of chromium is to produce a net increase in moment on the iron atoms around an impurity site, although the moment on the chromium atom is antiparallel to the host moment.<sup>2</sup> This magnetic-moment disturbance persists over a range of several near neighbors to an impurity.

More recently, similar experiments on ferromagnetic nickel-copper alloys<sup>3,4</sup> showed that these disturbance effects can be observed over an extended concentration range, and, as the critical concentration for the disappearance of ferromagnetism is approached, the range and magnitude of the disturbance become greater. These results implied that the moment of an individual atom depends on its local environment, in agreement with the variability of the average magnetic moments as a function of bulk concentration.

The iron-chromium system is one of only two Fe-base alloy series (the other is iron-vanadium) where a wide solid-solution range occurs in which

the concentration dependence of the magnetic moments can be conveniently studied. In Paper I,<sup>5</sup> the average magnetic moment per atom, as determined from bulk magnetization measurements, was presented as a function of composition. The classic neutron scattering experiments of Shull and Wilkinson<sup>6</sup> gave a measure of the 3*d* magnetic moments at the iron and chromium sites in iron-chromium alloys. The pronounced concentration dependence of these moments again implies the presence of local-moment-disturbance effects. In the present study, we have used long-wavelength, low-angle neutron scattering experiments to evaluate these disturbance effects and to reexamine the concentration dependence of the average moments.

## II. EXPERIMENTAL

The alloy samples were prepared by arc-melting the requisite amounts of 99.99-wt%-pure iron and chromium in a helium-argon mixture. Because the alloys are brittle at room temperature, the resultant buttons were rolled at ~850 °C to yield samples 5 mm thick, cut into pieces 3 cm square, annealed at 1150 °C for one week, and water quenched. Electron-microprobe analysis indicated that the samples were microscopically homogeneous, although the preparation techniques could not prevent some chemical short-range clustering in the samples as will be shown later.

The compositions of the alloys, as determined by chemical analysis, were 15.0-, 30.0-, 50.0-, and 73.0-at.% Cr.

The bulk magnetic moments of the samples, needed in the data analysis, were determined by magnetization measurements at 5 K; the experimental techniques have been described previously.<sup>7</sup> The moments of the 15-, 30-, and 50-at.% Cr samples were identical, within experimental error, with the values for separately prepared alloys given in Paper I.<sup>5</sup> The neutron scattering experiments were performed at 4.2 K on the Harwell diffractometer system mentioned earlier; experimental details are given in Ref. 3.

### III. RESULTS

#### A. Nuclear diffuse scattering

The nuclear component of the diffuse-scattering cross section for an alloy of composition  $\text{Fe}_{1-c}\text{Cr}_c$  may be written as

$$\left(\frac{d\sigma}{d\Omega}\right)_{\text{nucl}} = c\sigma_{\text{Cr}} + (1-c)\sigma_{\text{Fe}} + c(1-c)(b_{\text{Fe}} - b_{\text{Cr}})^2 S(\kappa), \quad (1)$$

where the  $\sigma$ 's are incoherent-scattering cross sections and the  $b$ 's are coherent-scattering lengths. The neutron scattering vector  $\kappa$  is defined as  $4\pi\lambda^{-1}\sin\theta$ , where  $\lambda$  is the neutron wavelength, and  $2\theta$  is the scattering angle. The  $S(\kappa)$  term is also present in the expression for the magnetic diffuse-scattering cross section and therefore must be evaluated independently. It is a measure of the chemical short-range nonrandomness in the alloy and is defined as

$$S(\kappa) = 1 + \sum_{R_i} N_i \alpha_i \sin\kappa R_i / \kappa R_i, \quad (2)$$

where  $R_i$ ,  $N_i$ , and  $\alpha_i$  are, respectively, the radius, coordination number, and short-range order parameter<sup>8</sup> of the  $i$ th near-neighbor atomic shell.

If the alloy is completely random, the  $\alpha$ 's are identically zero,  $S(\kappa) = 1$ , and the nuclear diffuse-scattering cross section is isotropic. This is not the case for the present alloys, as is seen in Fig. 1, which represents the nuclear cross section as a function of scattering vector for each of the alloys. If we take the accepted values for the incoherent cross sections ( $\sigma_{\text{Cr}} = 202$  and  $\sigma_{\text{Fe}} = 34$  in mb/sr atom) and the coherent-scattering lengths ( $b_{\text{Fe}} = 0.951$  and  $b_{\text{Cr}} = 0.352$  in  $10^{-12}$  cm), then  $S(\kappa)$  can be evaluated from the data in Fig. 1 by means of Eq. (1) and is shown as a function of  $\kappa$  in Fig. 2.

Attempts to least-squares fit the data of Fig. 2 to Eq. (2) were fraught with the same problems noted in Ref. 3, namely, large unphysical values

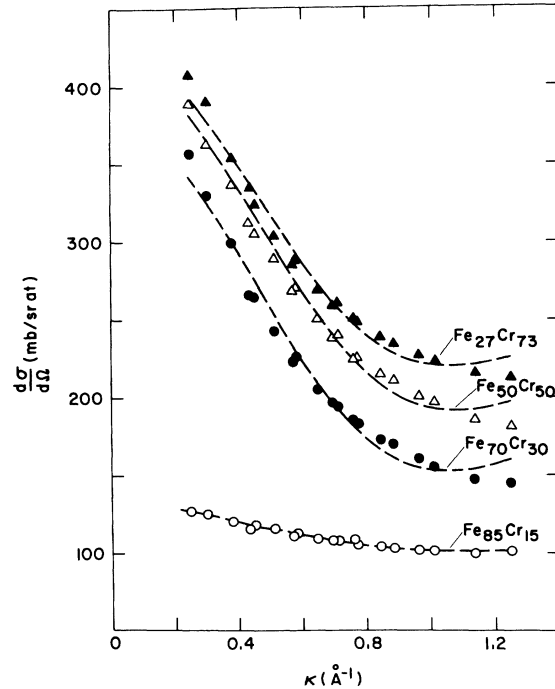


FIG. 1. Nuclear diffuse-scattering cross sections of Fe-Cr alloys as a function of scattering vector. The dashed lines represent least-squares analysis of the data (see text).

of  $\alpha_i$  of alternating sign for successive atomic shells were obtained. To provide additional constraints for the fitting process, a procedure found useful in Ref. 3 was employed, i.e., the minimization was made on the product of the root-mean-square (rms) error and  $\sum_{R_i} |N_i \alpha_i|$ . The results of this analysis, which was indistinguishable from an unconstrained fit on the scale of Fig. 2, are given in Table I and shown as the dashed lines in Figs. 1 and 2. It appears that Eq. (2) does not provide a good representation of the experimental data. The origin of this discrepancy may be associated with the restriction of the number of parameters to four. This is supported by the large contribution to  $S(\kappa)$  from  $N_4 \alpha_4$  (Table I), which effectively contains all the terms with  $i \geq 5$ . Unfortunately, an increase in the number of parameters intensifies the problems of constraining the fit.

The fact that  $S(\kappa)$  is greater than unity at small values of  $\kappa$  indicates short-range chemical clustering is present in Fe-Cr alloys quenched from high temperature. This clustering is consistent with the Fe-Cr phase diagram,<sup>9</sup> which shows a miscibility gap over a wide concentration range at temperatures below  $\sim 800^\circ\text{C}$ . The main contributions to  $S(\kappa)$  are from the generally positive  $\alpha_1$  and  $\alpha_4$ . Because of the problems in reproducing

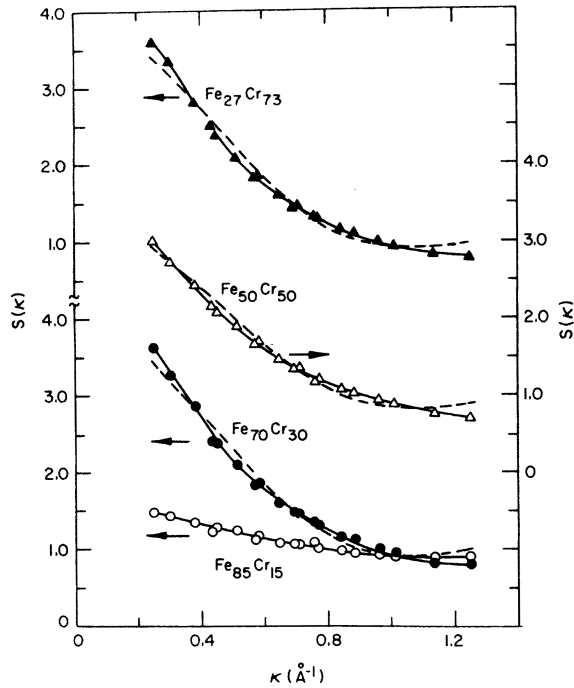


FIG. 2. Chemical short-range-order terms  $S(\kappa)$  as a function of scattering vector for Fe-Cr alloys. The dashed lines represent least-squares fits to Eq. (2). The solid lines are best fits drawn by eye. For the  $\text{Fe}_{85}\text{Cr}_{15}$  sample, the two lines are indistinguishable.

$S(\kappa)$  in an analytic form, best-fit lines were drawn by eye through the data in Fig. 2 (solid lines), and  $S(\kappa)$  values interpolated from these lines were used in the analysis of the magnetic cross sections.

### B. Magnetic diffuse scattering

The magnetic diffuse-scattering cross sections of the various alloys are shown in Fig. 3. To analyze these data, we use, following Ref. 3, the formalism of Marshall<sup>10</sup> and express the magnetic cross section (in mb/sr atom) as

$$\left(\frac{d\sigma}{d\Omega}\right)_{\text{mag}} = 48.6c(1-c)S(\kappa)f^2(\kappa)[M(\kappa)]^2, \quad (3)$$

where

$$M(\kappa) = \mu_{\text{Cr}} - \mu_{\text{Fe}} + (1-c)G(\kappa) + cH(\kappa) + (1-2c)[W(0) + W(\kappa)]. \quad (4)$$

In these expressions,  $f(\kappa)$  is the atomic  $3d$  form factor,  $\mu_{\text{Cr}}$  and  $\mu_{\text{Fe}}$  are the average  $3d$  magnetic moments in the absence of chemical short-range order,

$$G(\kappa) = \sum_{R_i} g_i N_i \frac{\sin \kappa R_i}{\kappa R_i}, \quad (5)$$

$$H(\kappa) = \sum_{R_i} h_i N_i \frac{\sin \kappa R_i}{\kappa R_i}, \quad (6)$$

and

$$W(\kappa) = \sum_{R_i} (h_i - g_i) \alpha_i N_i \frac{\sin \kappa R_i}{\kappa R_i}. \quad (7)$$

Here  $g_i$  is defined as the disturbance in the  $3d$  moment of an iron atom produced by each additional chromium atom at a distance  $R_i$ , and  $h_i$  is the corresponding disturbance in moment at a chromium atom. Because of the  $\alpha$  parameters in Eq. (7) and the concentration term in Eq. (4), it is anticipated that the contribution of  $W(0) + W(\kappa)$  to  $M(\kappa)$  [Eq. (4)] is small, as was found in the case of Ni-Cu alloys,<sup>3</sup> and this term will be neglected in the remainder of the analysis.

A major component of the  $\kappa$  dependence of the cross-section data shown in Fig. 3 arises from the  $S(\kappa)$  term that was evaluated earlier. The  $\kappa$  dependence of the atomic  $3d$  form factor was approximated by the expression  $f(\kappa) = 1.0 - 0.061\kappa^2$ , based on the calculated iron form factor of Freeman and Watson.<sup>11</sup> Values of  $M(\kappa)$  were then calculated, via Eq. (3), from the experimental cross sections (Fig. 3), and the results are shown in Fig. 4. The negative sign of  $M(\kappa)$  was fixed by the

TABLE I. Chemical short-range-order parameters for quenched Fe-Cr alloys determined from nuclear diffuse-scattering data.<sup>a</sup>

Conc. Cr	$\alpha_1$ $N_1=8$ $R_1 \approx 2.49 \text{ \AA}$	$\alpha_2$ $N_2=6$ $R_2 \approx 2.87 \text{ \AA}$	$\alpha_3$ $N_3=12$ $R_3 \approx 4.06 \text{ \AA}$	$\alpha_4$ $N_4=24$ $R_4 \approx 4.77 \text{ \AA}$	rms error
0.15	0.000(6)	0.015(9)	0.022(15)	0.009(6)	0.03
0.30	0.144(23)	0.000(33)	-0.045(53)	0.095(21)	0.12
0.50	0.075(15)	0.002(22)	0.054(35)	0.038(15)	0.08
0.73	0.138(19)	-0.001(26)	-0.023(41)	0.084(17)	0.10

<sup>a</sup> Numbers in parentheses represent statistical errors in the last significant figure(s) of the parameter.

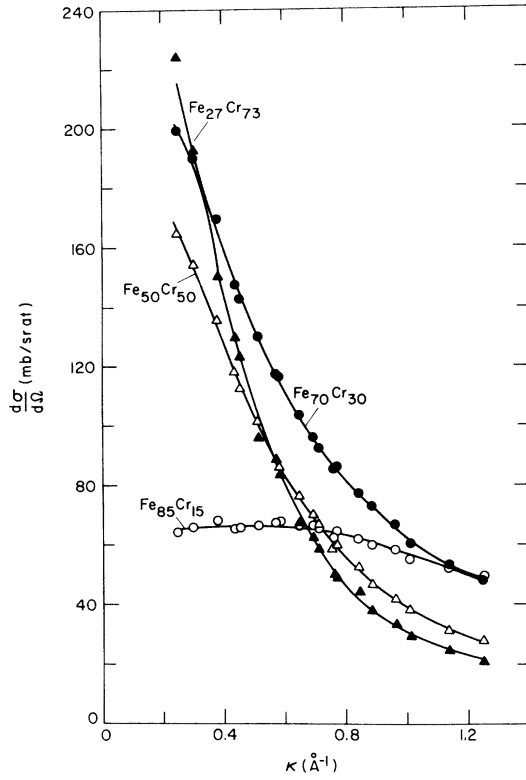


FIG. 3. Magnetic diffuse-scattering cross sections of Fe-Cr alloys as a function of scattering vector. The solid lines represent least-squares fits to the data (see text).

assumption that  $\mu_{\text{Fe}} > \mu_{\text{Cr}}$ .

It is possible to perform a least-squares analysis of the data shown in Fig. 4 in terms of Eq. (4). However, the simplifying assumption used in Ref. 3 that the moment on, in this case, the chromium atoms is negligible and  $H(\kappa)$  can be neglected is not justified.<sup>6</sup> Thus no way exists, *a priori*, to separate the individual  $g_i$  and  $h_i$  terms inasmuch as they have the same  $\kappa$  dependence. To simplify the Marshall formalism, we have replaced the term  $(1-c)G(\kappa) + cH(\kappa)$  by  $A(\kappa)$  so that, neglecting the  $W$  terms,

$$M(\kappa) \approx \mu_{\text{Cr}} - \mu_{\text{Fe}} + A(\kappa), \quad (8)$$

where

$$A(\kappa) = \sum_{R_i} a_i N_i \frac{\sin \kappa R_i}{\kappa R_i} \quad (9)$$

and

$$a_i = (1-c)g_i + ch_i. \quad (10)$$

The results of the least-squares analysis, in terms of Eqs. (8) and (9), are shown as the solid lines in Fig. 4, and some of the numerical values

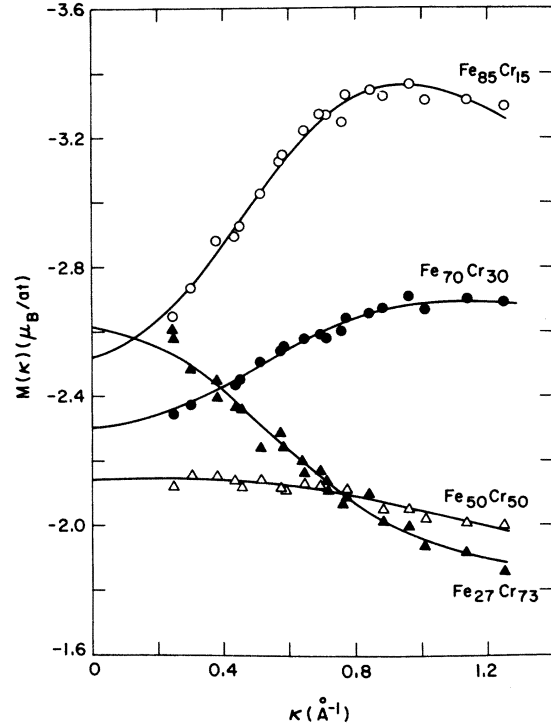


FIG. 4. Magnetic-moment density function  $M(\kappa)$  as a function of scattering vector for Fe-Cr alloys. The solid lines represent least-squares fits to the data (see text).

obtained are listed in Table II, including the results of an analysis of the data for an  $\text{Fe}_{98}\text{Cr}_2$  alloy that are presented in Fig. 1 of Ref. 2. Again, the minimization was performed on the product of the rms error and  $\sum_{R_i} |N_i a_i|$ . Even with this constraint, the individual  $a_i$  values for successive shells tend to have opposite signs and large uncertainty; therefore, they have not been given in Table II. The values of  $\mu_{\text{Cr}} - \mu_{\text{Fe}}$  and  $A(0)$  are well determined within the quoted uncertainty.

The concentration dependence of the moment difference  $\mu_{\text{Cr}} - \mu_{\text{Fe}}$  and the total disturbance  $A(0)$  are shown in Fig. 5; both vary smoothly but in opposite directions, as in the case of Ni-Cu alloys.<sup>3</sup> The dashed line represent values of  $\mu_{\text{Cr}} - \mu_{\text{Fe}}$  obtained from the results of a coherent-potential-approximation (CPA) calculation made for the Fe-Cr system by Frollani *et al.*<sup>12</sup>; the calculation will be considered in more detail in Sec. V. The solid line labeled  $d\langle\bar{\mu}\rangle/dc$  in Fig. 5 represents the concentration dependence of  $d\langle\bar{\mu}\rangle/dc$  obtained from bulk magnetization measurements (see Ref. 5), where  $\langle\bar{\mu}\rangle$  is the mean atomic moment of a real alloy with chemical short-range order. It can be deduced from Marshall's work<sup>9</sup> that

$$\frac{d\langle\bar{\mu}\rangle}{dc} = M(0) \approx \mu_{\text{Cr}} - \mu_{\text{Fe}} + A(0), \quad (11)$$

TABLE II. Parameters (in  $\mu_B$ ) obtained from analysis of magnetic diffuse-scattering cross sections of Fe-Cr alloys.

Cr Conc.	$\mu_{Cr}-\mu_{Fe}$	$A(0)$	$\langle\bar{\mu}\rangle$	$\mu_{Fe}$	$\mu_{Cr}$	$G(0)$	$H(0)$	$A(0)_{calc}$
0.02	-3.40	1.45	2.174 <sup>a</sup>	2.24	-1.16	1.23	2.01	1.25
0.15	-3.15	0.62	1.837	2.31	-0.84	0.08	2.95	0.51
0.30	-2.60	0.29	1.467	2.25	-0.35	-0.82	2.60	0.20
0.50	-2.10	-0.08	0.995	2.05	-0.05	-1.04	0.61	-0.22
0.73	-1.80	-0.83	0.475	1.80	0	-2.59	0	-0.70
Typical uncertainty	$\pm 0.10$	$\pm 0.15$	$\pm 0.001$	$\pm 0.10$	$\pm 0.10$	$\pm 0.25$	$\pm 0.25$	$\pm 0.25$

<sup>a</sup> Value given in Ref. 5.

and values of  $d\langle\bar{\mu}\rangle/dc$  calculated from the neutron data by means of Eq. (11) are seen to be in excellent agreement with the bulk magnetization results in Fig. 5; this provides an additional check on the reliability of the present data.

#### IV. DISCUSSION

The most striking feature of the results presented in the previous section, is the change in sign of the overall disturbance term  $A(0)$  as a function of concentration (Table II and Fig. 5). The long-range nature of this disturbance in dilute alloys of chromium in iron<sup>2</sup> is also evident in the concentrated alloys. However, the  $\kappa$  dependence of  $M(\kappa)$  (Fig. 4) indicates that the disturbance becomes shorter in range as the chromium concentration increases; this is borne out qualitatively by the individual  $a_i$  parameters; i.e.,  $a_1$  (which is negative) becomes more dominant as the chromium concentration increases.

Because the dependence of the magnetic moment of an individual atom on its environment is related to the concentration dependence of the average moment per atom, the change in local disturbance with concentration has implications with regard to the variation of  $\mu_{Fe}$  and  $\mu_{Cr}$  with composition. Although at first sight it may appear straightforward to determine  $\mu_{Fe}$  and  $\mu_{Cr}$  from the values of the moment-difference term (Table II) and the bulk magnetic moment (determined by magnetization measurements), a possible contribution to the bulk moment from a nonlocal polarization exists, which would make a contribution to the magnetic cross section only at  $\kappa$  values below the experimental range. The interpretation and fundamental significance of such a term in iron (and nickel) is still a subject of doubt.<sup>13,14</sup>

If such a nonlocal moment term  $\mu_{nl}$  is present in Fe-Cr alloys, which is essentially spatially invariant from site to site, then the total moment at an iron atom  $\mu_{Fe}^T = \mu_{Fe} + \mu_{nl}$ , and, correspondingly

$\mu_{Cr}^T = \mu_{Cr} + \mu_{nl}$ . It is then obvious that  $\mu_{Cr} - \mu_{Fe} = \mu_{Cr}^T - \mu_{Fe}^T$ , so that  $\mu_{Cr}$  and  $\mu_{Cr}^T$  and  $\mu_{Fe}$  and  $\mu_{Fe}^T$  can be treated as being formally identical. We may then write

$$\langle\bar{\mu}\rangle = (1-c)\mu_{Fe} + c\mu_{Cr}, \quad (12)$$

where it is understood that  $\mu_{Fe}$  and  $\mu_{Cr}$  are now the total moments per site, which may be evaluated without any assumptions as to the concentration dependence of  $\mu_{nl}$ .

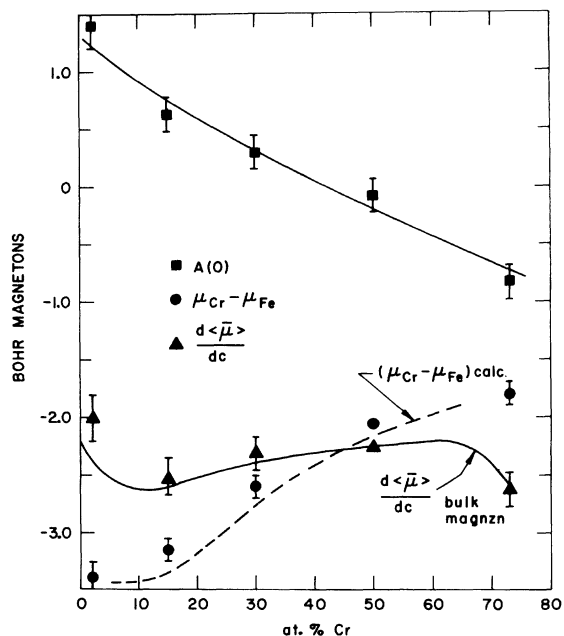


FIG. 5. Concentration dependence of parameters derived from an analysis of magnetic diffuse-scattering data for Fe-Cr alloys. Comparison is made with  $d\langle\bar{\mu}\rangle/dc$  obtained from bulk magnetization measurements (solid line) and  $\mu_{Cr} - \mu_{Fe}$  determined from a CPA calculation (dashed line) made for Fe-Cr alloys by Frollani *et al.* (Ref. 12). The line through the  $A(0)$  values is a guide to the eye.

The mean-magnetic-moment values  $\langle \bar{\mu} \rangle$  for the alloys are also listed in Table II together with values of the total moments  $\mu_{Fe}$  and  $\mu_{Cr}$  calculated from the moment-difference results and Eq. (12). The concentration dependence of the average magnetic moments at the iron and chromium sites is presented in Fig. 6. Also shown are values calculated by combining the data of Shull and Wilkinson<sup>6</sup> with mean moments interpolated from the results in Paper I, and values obtained in a polarized neutron study by Lander and Heaton.<sup>15</sup> Inasmuch as both of these sets of experiments were performed at room temperature, the results were normalized to 4.2 K by means of the temperature dependence of the mean moment at the relevant composition given in Ref. 5. The dashed lines represent the results of the CPA calculation of Frollani *et al.*<sup>12</sup> Numerical values for the spin-only moments were converted to total moment by means of the same  $g$  values used in Paper I.<sup>16</sup> The qualitative features of the experimental concentration dependence of the iron and chromium moments are well reproduced by the calculation. The differences in absolute magnitude may be associated with approximations in the calculation.<sup>12</sup>

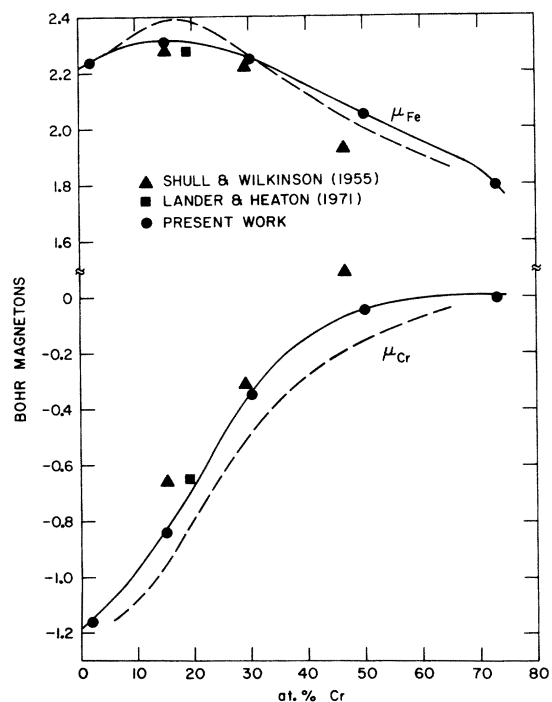


FIG. 6. Concentration dependence of the average magnetic moments at the iron and chromium sites in Fe-Cr alloys. The dashed lines are the results of a CPA calculation by Frollani *et al.* (Ref. 12). The solid lines are best fits drawn by eye (see text).

The moment-difference term given by the CPA calculation (dashed line labeled  $\mu_{Cr} - \mu_{Fe}$  in Fig. 5) is almost in quantitative agreement with the neutron-scattering data.

An additional consequence of the Marshall formalism<sup>3,10</sup> used in the data analysis is that  $d\mu_{Fe}/dc = G(0)$  and  $d\mu_{Cr}/dc = H(0)$ . Therefore, the concentration dependence of  $\mu_{Fe}$  and  $\mu_{Cr}$  must be consistent with the concentration dependence of the disturbance term inasmuch as, from Eq. (10),

$$A(0) = (1 - c)G(0) + cH(0). \quad (13)$$

This feature provides a powerful check on the internal self-consistency of the results. The solid lines through the present experimental values of  $\mu_{Fe}$  and  $\mu_{Cr}$  were hand drawn to give slopes, at each concentration, consistent with Eq. (13) and the experimental values of  $A(0)$ . The graphically determined derivatives obtained from these lines are listed as  $G(0)$  and  $H(0)$  in Table II, together with values of  $A(0)$  calculated from Eq. (13). Because two unknowns and one variable are involved, the  $G(0)$  and  $H(0)$  values should be treated cautiously; however, the general qualitative features are valid. In particular, the change in sign of  $A(0)$  with concentration appears to reflect the corresponding change in the sign of  $G(0)$  (Table II and Fig. 6). In dilute alloys of chromium in iron,<sup>2</sup> the isolated chromium impurity atom reduces the iron moments at the nearest neighbor (the value of  $a_1$  is negative as noted earlier) and increases the iron moments at greater distances. This occurs primarily as a result of charge screening by majority-spin carriers.<sup>1</sup> In a concentrated alloy, where each iron atom experiences much the same average long-range environment, the magnitude of the iron moment is apparently determined primarily by its local nearest-neighbor surroundings. Thus, the range of the total disturbance appears to be shorter in the more chromium-rich alloys (Fig. 4). In view of the itinerant nature of the magnetic electrons in chromium, we would expect that the chromium-chromium interactions [as given by  $H(0)$ ] would be long range. The concentration dependence of  $H(0)$  (Table II) would indicate that this interaction is more important in the Fe-rich alloys where the chromium moments are relatively large.

The moments in Fig. 6 should, in principle, extrapolate to zero at the critical concentration where ferromagnetism disappears, which in the Fe-Cr system is near 80-at.% Cr.<sup>17-19</sup> This would imply a rapid decrease in the average iron moment beyond 73-at.% Cr (Fig. 6) and consequently a rapid increase in the negative disturbance term  $G(0)$ . A similar effect was observed in Ni-Cu alloys<sup>3,4</sup> where the presence of giant polarization

clouds was detected at compositions near the critical composition.<sup>4</sup> By analogy, we would expect similar polarization clouds to be present in Fe-Cr alloys; the critical magnetic properties of alloys in this concentration region give evidence of the presence of polarization clouds.<sup>20</sup>

#### V. SUMMARY

Diffuse-neutron-scattering techniques have been used to determine both the average moments at chromium and iron sites in Fe-Cr alloys and the disturbances in individual moments caused by variations in local environment. The pronounced concentration dependence of both  $\mu_{Fe}$  and  $\mu_{Cr}$  reflects changes in the nature of the disturbances with concentration. It is argued that the distur-

ance in moment at chromium atoms is long range in nature, whereas the long-range disturbance in moment at iron atoms in iron-rich alloys gives way to a more local disturbance as the chromium concentration increases. In the critical concentration region where ferromagnetism disappears, we would anticipate the presence of polarization clouds.

#### ACKNOWLEDGMENTS

We would like to thank Dr. G. G. Low of Harwell for use of the facilities and many helpful discussions and Dr. F. Y. Fradin for critically reading the manuscript. We acknowledge the capable experimental assistance of V. Rainey.

---

\*Work supported by the U. S. Energy Research and Development Administration and the United Kingdom Atomic Energy Authority.

<sup>1</sup>G. G. Low, *Adv. Phys.* **18**, 371 (1969), and references therein.

<sup>2</sup>M. F. Collins and G. G. Low, *Proc. Phys. Soc. Lond.* **86**, 535 (1965).

<sup>3</sup>A. T. Aldred, B. D. Rainford, T. J. Hicks, and J. S. Kouvel, *Phys. Rev. B* **7**, 218 (1973).

<sup>4</sup>T. J. Hicks, B. D. Rainford, J. S. Kouvel, G. G. Low, and J. B. Comly, *Phys. Rev. Lett.* **22**, 531 (1969).

<sup>5</sup>A. T. Aldred, preceeding paper, *Phys. Rev. B* **14**, 219 (1976).

<sup>6</sup>C. G. Shull and M. K. Wilkinson, *Phys. Rev.* **97**, 304 (1955).

<sup>7</sup>A. T. Aldred, *J. Appl. Phys.* **37**, 671 (1966); and *J. Phys. C* **1**, 244 (1968).

<sup>8</sup>J. M. Cowley, *Phys. Rev.* **77**, 669 (1950).

<sup>9</sup>M. Hansen, *Constitution of Binary Alloys* (McGraw-Hill, New York, 1958).

<sup>10</sup>W. Marshall, *J. Phys. C* **1**, 88 (1968). See also Ref.

3 and notes therein for a more detailed exposition of the analysis.

<sup>11</sup>A. J. Freeman and R. E. Watson, *Acta Crystallogr.* **14**, 231 (1961).

<sup>12</sup>G. Frollani, F. Menzinger, and F. Sacchetti, *Phys. Rev. B* **11**, 2030 (1975).

<sup>13</sup>W. Marshall and S. W. Lovesey, *Theory of Thermal Neutron Scattering* (Oxford U. P., London, 1971), p. 181.

<sup>14</sup>K. J. Duff and T. P. Das, *Phys. Rev. B* **3**, 2294 (1971).

<sup>15</sup>G. H. Lander and L. Heaton, *J. Phys. Chem. Solids* **32**, 427 (1971).

<sup>16</sup>P. David and M. Heath, *J. Phys. (Paris)* **32**, C1-112 (1971).

<sup>17</sup>R. D. Shull and P. A. Beck, *AIP Conf. Proc.* **24**, 95 (1975).

<sup>18</sup>B. Loegel, J. M. Friedt, and R. Poinot, *J. Phys. F* **5**, L54 (1975).

<sup>19</sup>Y. Ishikawa, R. Tournier, and J. Filippi, *J. Phys. Chem. Solids* **26**, 1727 (1965).

<sup>20</sup>A. T. Aldred (unpublished).